Electrodeposition of Poly(*N*-vinylcarbazole) at the Three-Phase Junction. Formation of Very Different Polymer Structures

Elzbieta Bak, Mikolaj Donten, Magdalena Skompska, and Zbigniew Stojek*

Department of Chemistry, Warsaw University, ul. Pasteura 1, PL-02-093 Warsaw, Poland

Received: June 23, 2006; In Final Form: September 24, 2006

Poly(*N*-vinylcarbazole) films can be deposited at the three-phase boundary when the organic phase contains only monomer, *N*-vinylcarbazole, while the aqueous phase contains supporting electrolyte. A cylindrical platinum microelectrode is immersed into the two-liquid system in such a way that a part of it is located in one liquid and the other part resides in the second liquid. The thickness of the reaction layer, or the width of the microelectrode zone where the polymer grows, depends on the kind of ions present in the aqueous phase and the time of the experiment. The structure of the deposited polymer may be very different and depends on the distance from the three-phase boundary and the type of the anion present in the aqueous phase. The key parameters here are the local electrode potential and the local concentration of the anions. The list of obtained polymer structures includes, among others, arrays of perfectly arranged deep oval channels and groups of microcrystals. The porosity of the polymer deposits increases with the distance from the aqueous phase.

1. Introduction

The term three-phase electrode most frequently refers to the experiments involving a solid working electrode being in direct contact with two immiscible liquid phases. The measurements with the use of three-phase electrodes were mainly directed at the investigation of the thermodynamics of ion transfer from one solvent (water) to another (organic). This was accomplished in several ways. One very popular configuration is based on the application of one[1,2] or more[3−6] droplets of organic liquid attached to the surface of a graphite electrode and immersed into an aqueous solution of appropriate ions. Either the pure organic solvent of the drop or an electroactive compound dissolved in it is subsequently reduced or oxidized. Reaction starts at the circumference of the organic droplet placed on the electrode surface, where the three phases meet and where the substrate, the counterions, and the electrons are available. The fact that the electrochemical reaction is initially confined to the three-phase boundary was experimentally proved by either doing the metal electrodeposition at the three-phase boundary,[7,8] or fitting the experimental current into appropriate theoretical relations,[9,10] or inserting a microelectrode probe into the organic droplet immobilized on the surface of a graphite disk.[11] It is now clear that while the electrochemical reaction advances in time, the reaction zone expands continuously toward the organic bulk.

Other experimental configurations for studying the ion transfer have also been successively utilized. They include, for example, the formation of three-phase junctions on the surface of electronically conductive particles such as carbon paste and porous ceramic phases,[12−15] and the use of micro- and nanopipets.[16] Our recent approach is based on immersing a gold or platinum microcylindrical electrode into a two-solvent system in such a way that the upper part of the wire remains in the aqueous phase and the lower part stays in the organic phase.[17] Obviously, both liquids must be immiscible. We believe that that approach is advantageous vs the other three-phase designs, since it offers a very reproducible size of the three-phase boundary which is located along the circumference of the wire. In consequence, that system provides an improved reproducibility of the magnitudes of the current responses, an easily controllable length of the three-phase junction by using metal wires of various diameters, and a possibility of employing various electrode materials and organic phases.

In this paper, we present the three-phase electrooxidation of the *N*-vinylcarbazole monomer that is present only in the supporting-electrolyte-free organic phase. The electrooxidation induces the electropolymerization of the monomer (poly(*N*-vinylcarbazole), PVCz, is formed) on the surface of the metal microwire at the three-phase junction. Electrochemical polymerization at a liquid/liquid interface has been reported already in the literature for, e.g., 2,2′:5′,2″-terthiophene.[18] The process at the three-phase boundary requires the presence of anions that must be brought from the aqueous phase. In the previous paper we have shown how the polymeric film grows along the Pt microwire toward the organic phase and marks this way the expansion of the reaction zone.[19] Now, we present how strongly the structural pattern of the polymer changes in time, in the presence of different anions incorporated, and with the distance from the three-phase boundary.

2. Experimental Section

Voltammetric and chronoamperometric measurements were performed using a model 273 EG&G PARC potentiostat controlled via a personal computer. The cell was enclosed in a Faraday cage to minimize electrical interferences. A Ag/AgCl/saturated KCl electrode was used as the reference electrode, and a platinum wire served as the auxiliary electrode. A platinum cylindrical electrode of 300 μm in diameter was used as the working electrode.

The following salts, lithium perchlorate ($LiClO_4$, 99%), tetrabutylammonium perchlorate (TBAP), tetrabutylammonium tetrafluoroborate, tetrabutylammonium hexafluorophosphate,

* To whom correspondence should be addressed. E-mail: stojek@chem.uw.edu.pl.

10.1021/jp063935w CCC: $33.50
Published on Web 11/11/2006

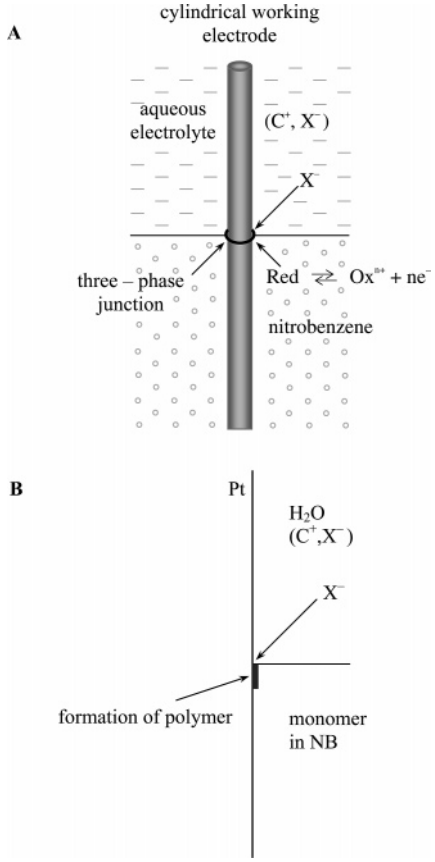

Figure 1. (A) Three-phase electrochemical cell. (B) Site of the polymerization process.

sodium trifluoromethanesulfonate (CF_3SO_3Na, 97%), sodium tetrafluoroborate ($NaBF_4$, 99%), sodium chlorate ($NaClO_3$), potassium bromate ($KBrO_3$), sodium iodate ($NaIO_3$), and sodium nitrate ($NaNO_3$) were purchased from Fluka and were used as supporting electrolytes in the aqueous phase. *N*-Vinylcarbazole was also purchased from Fluka. Nitrobenzene was supplied by Aldrich and was saturated with water before experiments. The aqueous electrolyte solutions were saturated with nitrobenzene and were prepared using high-purity water obtained from a Milli-Q Plus/Millipore purification system (conductivity of water, 0.056 mS cm^{-1}). The surface structure of the PVCz films was monitored with an Optymus optical microscope equipped with a camera, and a LEO, model 435 VP, scanning electron microscope integrated with a Roentec EDX analyzer. All experiments were performed at 22 °C.

3. Results and Discussion

The experimental setup for the three-phase electrode approach with a cylindrical microelectrode is presented in Figure 1A. In this case the three-phase boundary and the initial reaction layer have the shape of a ring with the inner diameter equal to that of the microwire. Figure 1B illustrates where the polymer is formed.

A typical set of five consecutive cyclic voltammograms obtained just in nitrobenzene alone containing the *N*-vinylcarbazole monomer and supporting electrolyte (TBAP) at concentrations of 0.01 and 0.1 M, respectively, is presented in Figure 2. The course of the voltammograms is characteristic of polymer electrodeposition on the working electrode surface. A strong increase in the current at the potentials higher than 1.1 V (A_2) results from the oxidation of the monomer to the radical cation. A pair of peaks (A_1/C_1) located in the potential range from 0.75

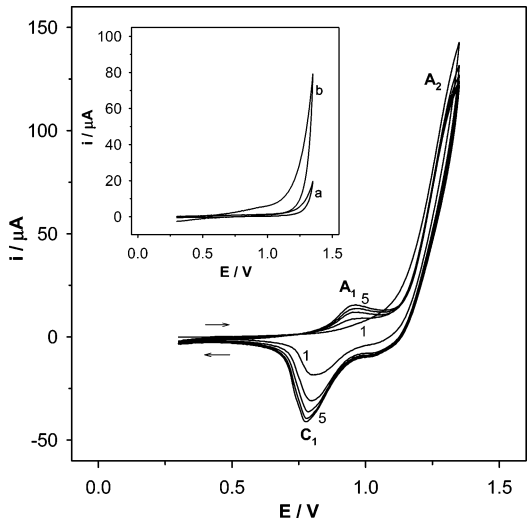

Figure 2. Cyclic voltammograms representing potentiodynamic electropolymerization of poly(*N*-vinylcarbazole) in nitrobenzene alone. Nitrobenzene contains monomer (*N*-vinylcarbazole) and TBAP at concentrations of 0.01 and 0.1 M, respectively. Conditions: Pt cylindrical microelectrode, 300 μm in diameter; potential scan rate, 50 mV/s. Numbers in the plot correspond to consecutive scans. (Inset) Three-phase system: nitrobenzene contains only 0.01 M monomer and is in contact with 1 M aqueous solution of $LiClO_4$ (curve b). Curve a represents the background.

SCHEME 1: Electrooxidation of Poly(*N*-vinylcarbazole)[a]

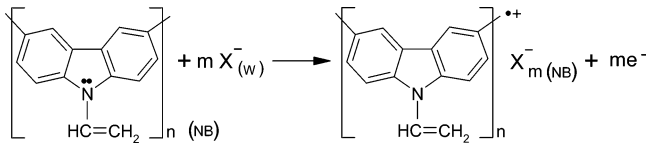

[a] Electrooxidation of poly *N*-vinylcarbazole, *m* is significantly smaller than *n*.

to 0.9 V corresponds to the oxidation and the reduction of the polymer already formed on the electrode surface. The cathodic peak C_1 is higher than the anodic one (A_1), probably due to the reduction of some soluble oligomers present near the electrode.

Figure 2 presents also, in the inset, the first voltammogram obtained in the three-phase system with no supporting electrolyte in the nitrobenzene phase (curve b). A strong increase of the current with respect to the background signal (curve a) is an indication of the monomer oxidation. However, the consecutive curves are very similar to the first scan; i.e., the polymer redox peaks do not increase in the subsequent scans. This means that under these specific conditions there is no growth of the polymer layer in the nitrobenzene phase. This situation is related to the fact that the film growth must be accompanied by the accumulation of counterions (anions) to neutralize the extra charge of the radical cations generated upon polymer oxidation; see Scheme 1. Simply, in the three-phase-electrochemistry, under cyclic voltammetric conditions, the process of increasing the anion concentration in the nitrobenzene phase is of too small efficiency and cannot support sufficiently the polymerization process. In other words, the time scale of the experiment performed by cyclic voltammetry (and especially the time at the electrooxidation region, where the anions are drawn) is too short to allow the formation of a significant amount of the polymer on the electrode surface. To extend the time scale of experiment, the polymer was deposited under constant-potential conditions (continuous electrooxidation of the monomer), which guaranteed a continuous supply of the anions to the reaction zone.

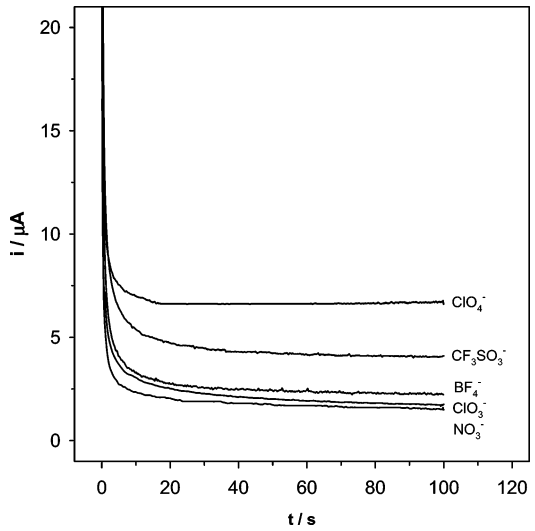

Figure 3. Chronoamperograms of oxidative polymerization of *N*-vinylcarbazole obtained at platinum cylindrical microelectrode. Conditions: 0.01 M *N*-vinylcarbazole in nitrobenzene, 1 M aqueous solutions of different salts, and electrode potential of 1.32 V vs Ag/AgCl. Other conditions as in Figure 2.

The oxidation of the monomer under three-phase conditions (including the nitrobenzene phase) occurs similarly to the process performed in acetonitrile alone. This conclusion is based on a comparison of oxidative chronoamperograms (not shown here) obtained for different potentials in both solvents. The electrooxidation of the monomer leads to the formation of the radical cation which binds to another radical cation or a neutral monomer molecule to form dimers, trimers, and finally the conductive polymer.[20−25] In acetonitrile, the polymerization via the vinyl groups has also been detected and the corresponding nonconducting white precipitate was obtained. That path of the polymerization was never found by us in nitrobenzene. Thus, very likely the vinyl groups are not involved in the polymerization process.

During the constant-potential experiments at the three-phase boundary, a Pt cylindrical electrode was immersed in the water/nitrobenzene system in the presence of various salts in the aqueous phase. The organic phase contained only *N*-vinylcarbazole monomer and the saturation level of water. A potential of +1.32 V was imposed to the Pt electrode for 100 s to ensure the successful polymerization of the monomer. It should be emphasized that the potential of +1.32 V was optimal for providing a sufficient polymerization rate: it was low enough to avoid the polymer degradation, the loss of its electroactivity,[26] and the decomposition of water. As it has been mentioned above, the electropolymerization in the organic phase is accompanied, to maintain the electroneutrality in the nitrobenzene zone where the polymer is formed, by the transport of appropriate supporting anions from the aqueous phase. This transport of anions is not limited by the anion-transfer potentials, since the applied polymerization potential is substantially more positive than each of the corresponding transfer potentials; see data in, e.g., reference 1. Therefore, the investigation of the film growth in the presence of various anions in the aqueous phase provides information on the ability of a particular anion to move in substantial quantities toward the organic phase bulk along the Pt microwire. However, there is a restriction in the choice of the anions for the polymerization process. They should be inert toward the radical cations present in the polymerization zone. For example, for many polymers, good films of high electroactivity are not formed in halides because of their nucleophilic character and because they are easily oxidized in the potential

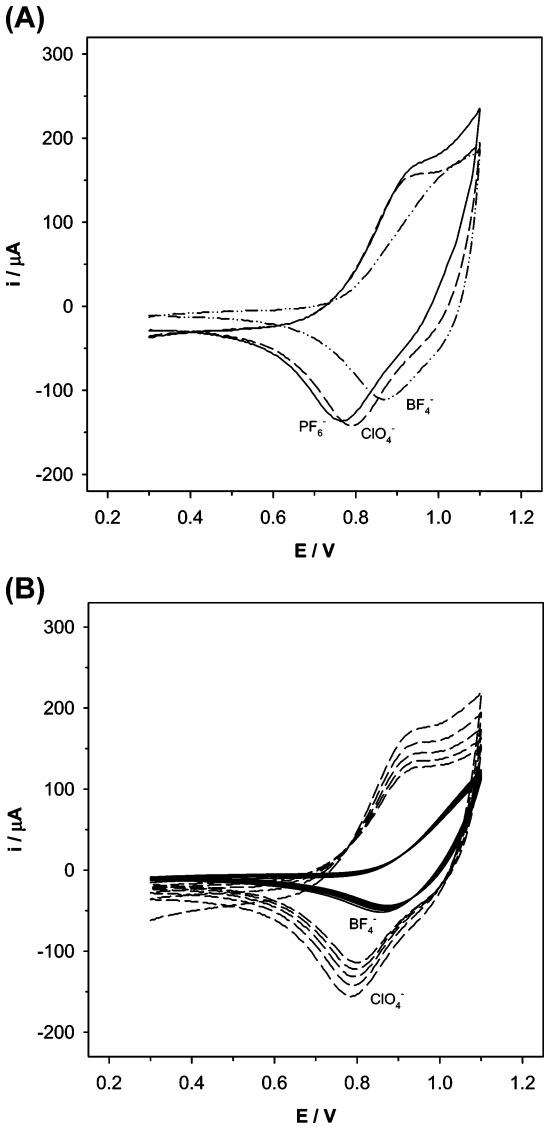

Figure 4. (A) Cyclic voltammograms of poly(*N*-vinylcarbazole) films in 0.1 M solutions of $TPAPF_6$, $TPAClO_4$, and $TBABF_4$ in nitrobenzene. (B) Cyclic voltammograms of poly(*N*-vinylcarbazole) films obtained in a nitrobenzene solution containing $TPAClO_4$ and transferred to a solution of the same anion (dashed curve) and to a solution of $TBABF_4$ (solid line). Pt cylindrical microelectrode of 300 μm in diameter (potential scan rate, 50 mV/s).

range of the electropolymerization.[27,28] Therefore, the investigated anions included the following: perchlorate, trifluoromethanesulfonate, tetrafluoroborate, chlorate, bromate, iodate, and nitrate.

The anion-intercalated polymer grew along a microwire outward from the phase boundary toward the nitrobenzene bulk. The rate of growth was expected to be dependent on the nature of the incorporated anions.[19] The highest rate should be obtained, from the thermodynamic point of view, for the most hydrophobic anions which should appear in the reaction zone at sufficiently high concentrations most easily. To confirm this, we have recorded chronoamperograms corresponding to oxidative polymerization of *N*-vinylcarbazole in the presence of the above anions. In the presence of perchlorate anions the largest current intensity was measured and the polymerization process was the most advanced. In contrast to ClO_4^-, the nitrate anion has the weakest affinity toward nitrobenzene and the corresponding current response was strongly decreased. Exemplary chronoamerometric responses obtained in the presence of the

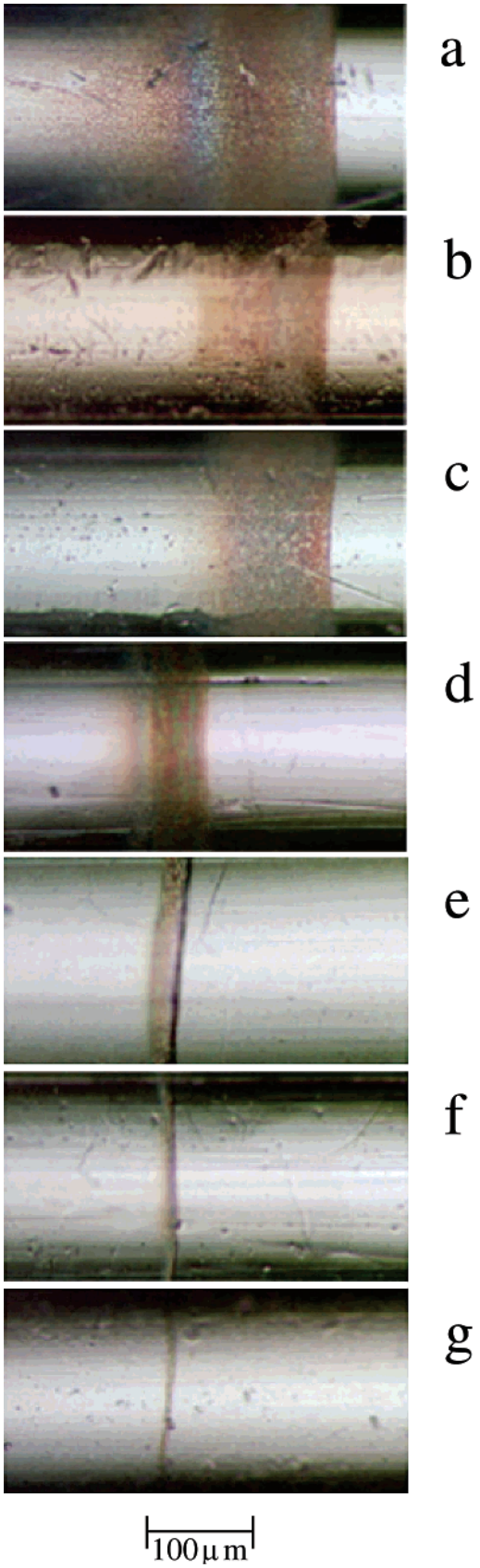

Figure 5. Microscopic images of polymer layers deposited at the three-phase boundary in the presence of various anions in the aqueous phase: 1 M ClO_4^- (a), 1 M $CF_3SO_3^-$ (b), 1 M BF_4^- (c), 0.5 M ClO_3^- (d), 0.5 M BrO_3^- (e), 0.5 M IO_3^- (f), and 1 M NO_3^- (g). Deposition time, 100 s; deposition potential, 1.32 V.

ClO_4^-, $CF_3SO_3^-$, BF_4^-, ClO_3^-, and NO_3^- anions are shown in Figure 3. They are in accordance with our earlier paper.[19] It is important to realize that each examined anion has a specific influence on the propagation of the polymerization reaction. As it was mentioned above, a possibility that the selected electropolymerization potential could be insufficiently positive for some anions to draw them from the aqueous phase and to do the polymerization can be rejected, since the applied polymerization potential was substantially higher than the potentials of ion transfer for all employed anions. It should be added here that the polymer layers obtained in nitrobenzene did not show any electroactivity after the transfer to the aqueous phase. There were no peaks on the voltammograms and no change in the polymer volume, which indicates that the polymer is not solvated by water.

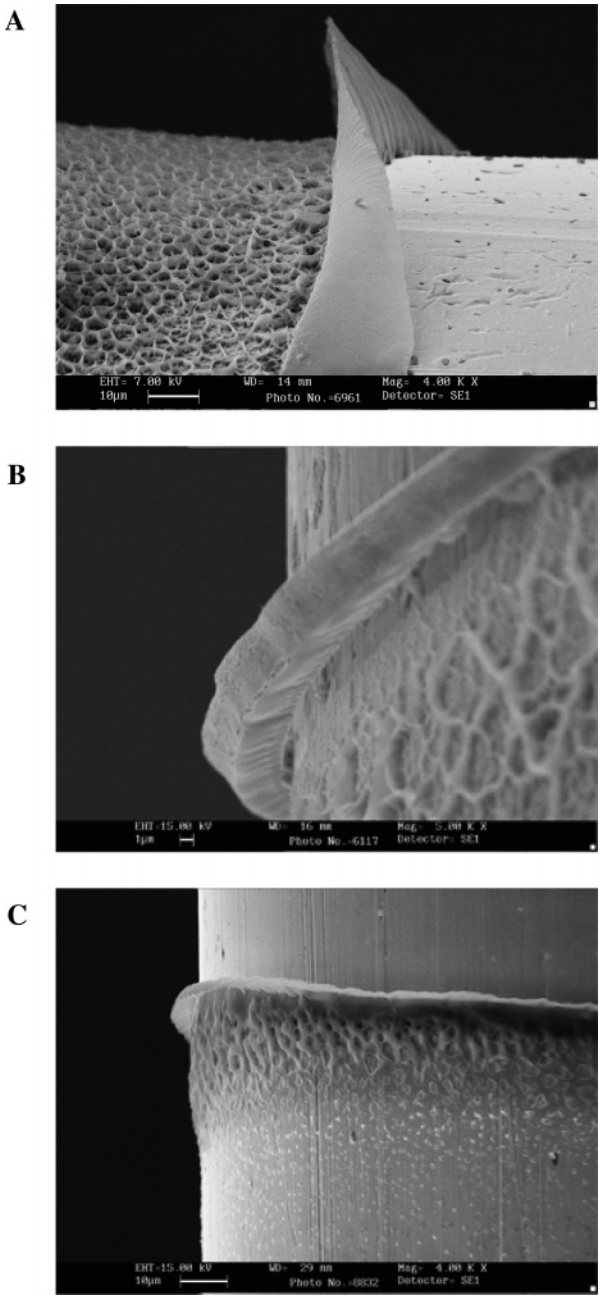

Figure 6. SEM micrographs of polymer deposits on Pt microcylinder located at the three-phase junction: concentration of monomer (*N*-vinylcarbazole), 0.01 M; deposition potential, 1.32 V; deposition time, 3600 s. Aqueous phase: (A) 1 M $LiClO_4$, (B) 0.5 M $KBrO_3$, and (C) 1 M $NaNO_3$.

Other parameters, not directly related to the three-phase conditions, that influence the polymerization process are the

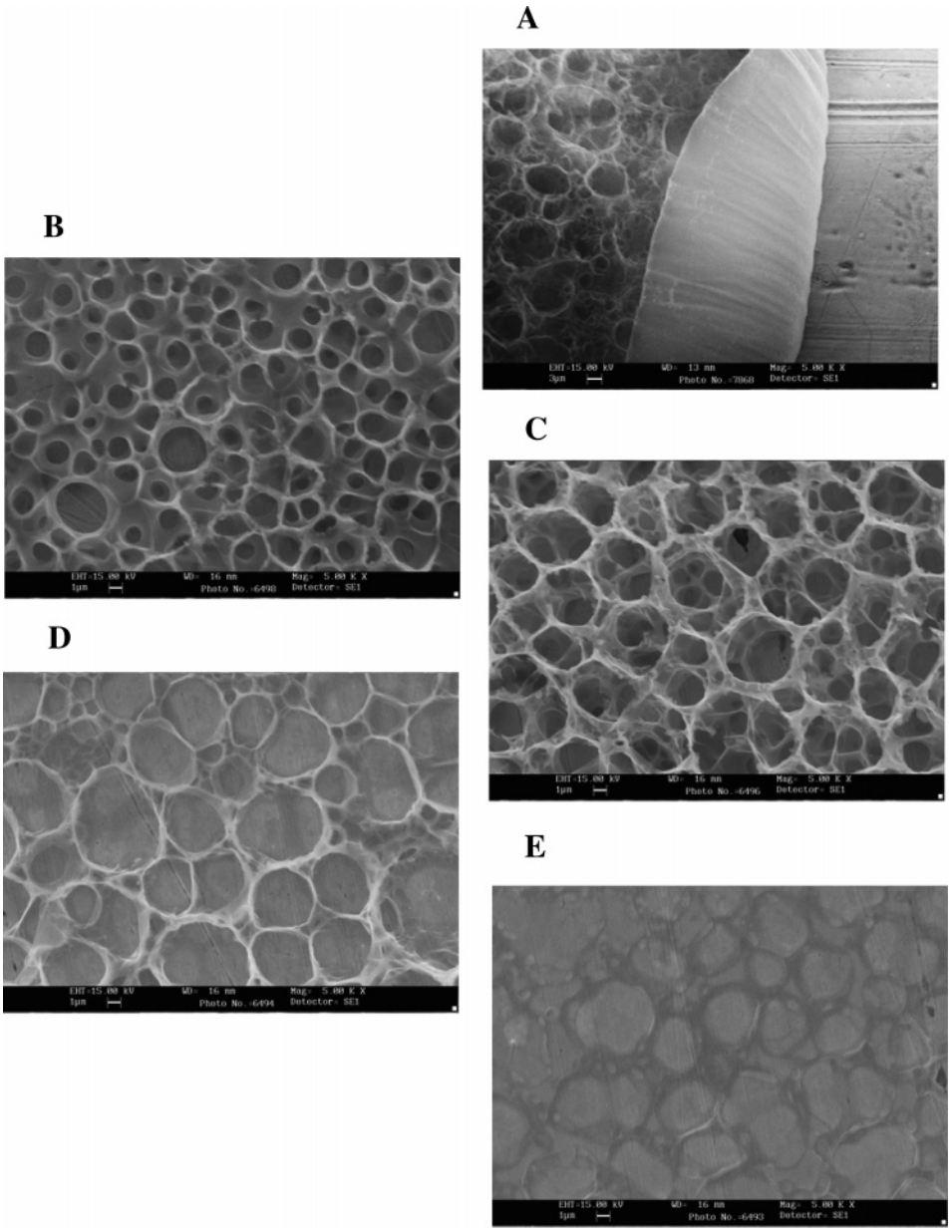

Figure 7. SEM micrographs of polymer deposits on Pt microcylinder located at different distances from the three-phase boundary: 15 (A), 55 (B), 120 (C), 200 (D), and 275 μm (E). NB (*N*-vinylcarbazole)/water (1 M ClO_4^-). Magnification: 5000 (B−E); 2000 (A). Cylinder diameter, 300 μm; deposition time, 250 s.

geometry and size of the doping anion. They may influence both the polymer morphology and its conductivity.[29] For example, $CF_3SO_3^-$ is a cylindrical ion (2.6 × 2.8 Å) carrying a highly delocalized charge, whereas ClO_4^- and PF_6^- are spherical non-coordinating ions. The ion size decreases in the following sequence: PF_6^- (3.01 Å) > ClO_4^- (2.9 Å) > BF_4^- (2.84 Å).[30] The film growth along the cylindrical Pt electrode may be dependent not only on the ease of penetration of nitrobenzene phase but also on the rate of propagation of anions in the polymer film. The anion transfer along the film may facilitate the polymerization at relatively long distance from the water−organic phase boundary. The smaller anions have higher mobility in the polymer matrix, and, therefore, the rate of the polymer growth and polymer conductivity should be higher than those in the case of larger anions. However, Lacaze et al. have shown (for regular electrodes and a single liquid phase) that the PVCz film growth in a ClO_4^- acetonitrile solution was faster than that in the presence of BF_4^- and PF_6^-. That took place while the ion transport through the polymer films of the same thickness was nearly the same in the three electrolytes examined.[22,23] On the other hand, the polypyrrole films obtained in aqueous ClO_4^- solutions revealed higher conductivities than those of the films obtained in the presence of the smaller NO_3^- ions.[31] Another phenomena that might influence the electropolymerization process is the formation of ion pairs in the organic phase. This has been especially checked by us in the case of formation of semicrystals.

The polymer films obtained in a nitrobenzene solution containing excess supporting electrolyte were very similar to those obtained in acetonitrile.[24,32] The structure was dense, and the surface contained many bumps. To examine the influence of anions on the electroactivity of the polymer, the microcylinder with the polymer deposit was transferred to a nitrobenzene solution containing the same anion and no monomer. The cyclic voltammetric curves obtained are presented in Figure 4A. It is clearly seen that the curve that is located at the least positive potential is obtained for PF_6^-. The most positive curve is that obtained in the presence of the BF_4^- anion. The PF_6^- anion is

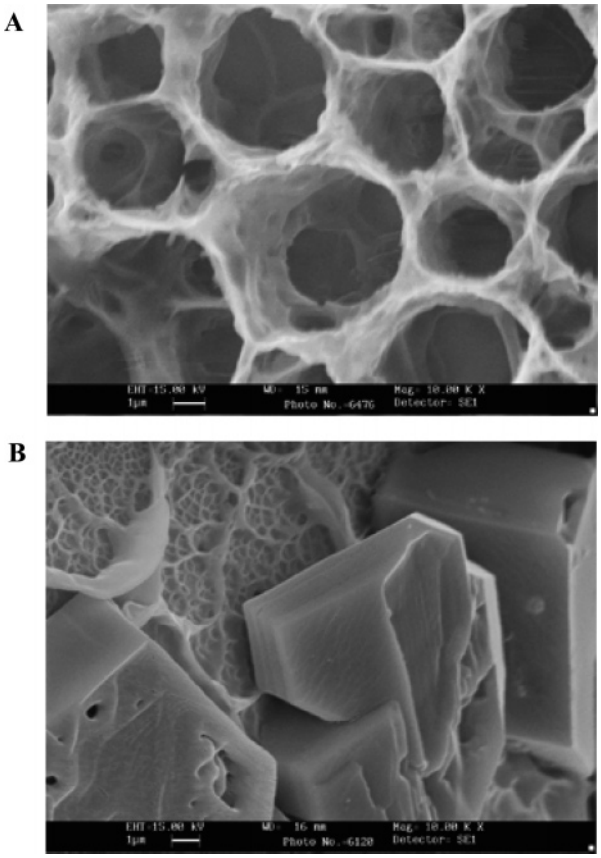

Figure 8. SEM micrographs of polymer deposits taken behind the collar: (A) 1 M $LiClO_4$ in the aqueous phase, 120 μm from the three-phase boundary; (B) 0.5 M $KBrO_3$ in the aqueous phase, next to the three-phase boundary.

the largest one and BF_4^- is the smallest; therefore, we think that specific interactions between the polymer cation radicals with anions are responsible for the potential change. This may also influence the channel/hole sizes within the polymer deposit. Indeed, interestingly, when the polymer layer obtained in the presence of one anion was placed in a nitrobenzene solution containing a different anion, the polymer deposit lost much of its electroactivity. An example is given in Figure 4B.

The width of the polymer film that was grown along the Pt microwire in the nitrobenzene phase during 100 s decreases in the sequence $ClO_4^- > CF_3SO_3^- \approx BF_4^- \gg ClO_3^- \gg BrO_3^- > IO_3^- > NO_3^-$. Typical images of the polymer deposits obtained for seven anions after a 100-s electrolysis on the surface of a Pt cylindrical electrode in the vicinity of the water/nitrobenzene boundary are presented in Figure 5. The polymer deposit grew progressively toward the organic phase with an increase in the lipophilicity of the charge-balancing anions. The greatest expansion of the polymer layer was observed for the perchlorate anion. In the presence of nitrates in the aqueous phase the film deposition was practically limited to a several-micrometer zone at the three-phase boundary. This behavior cannot be explained by just different mobility of the ions inside the polymer film. It is an evident result of very different ability of penetration of the ions into the organic phase.

It is worth noting that the width of the polymer layer formed with the aqueous phase containing BF_4^- is relatively wide, compared to that obtained for ClO_4^- and $CF_3SO_3^-$, whereas the current intensity measured during the potentiostatic deposition was much lower. One possible explanation for this is that the thickness of the polymer films obtained in the presence of various anions is different and the yields of the polymerization processes are different. Another explanation can be offered after inspecting the SEM micrographs of the films: the polymer grew not only along the Pt wire but also perpendicularly to the electrode surface to form a collar around the Pt wire just at the boundary between water and nitrobenzene; see Figure 6.

The morphology of the poly(*N*-vinylcarbazole) layers is apparently related to the environment of the polymerization reaction. It is known that the highest morphological homogeneity of the poly(*N*-vinylcarbazole) was observed in a mixture of organic solvent and water.[24,32] In a nonaqueous media the polymer becomes porous. In our investigations, precisely at the water−nitrobenzene boundary, where both solvents are available, the surface of the polymer is smooth (see Figure 6). In fact, the polymer deposits are seen as smooth rings/collars of various thicknesses and widths. The collar can be either very thin, of a foil type, or pretty rigid. As the distance from the liquid-phase−liquid-phase boundary increases, the porosity of the polymer increases significantly. This is illustrated in Figure 7. Porosity is the largest just behind the collar, where the diameter of the rings changes from 2 to 6.6 μm (please note that the magnification in Figure 7A is smaller compared to micrographs B−E). Further behind the collar the diameter diminishes ($1 \div 4.5$ μm, Figure 7B), then increases again, and finally reaches the range of $3 \div 8$ μm at the end of the deposit (Figure 7E). The structural changes shown in Figure 7A−E must be a result of three factors: unavailability of water, insufficient concentration of anions, and a drop in the local electrode potential (substantial ohmic drop exists in the organic phase). The availability of the anions can be strongly limited not only at the end of the polymer deposit but as well just behind the collar, which forms a kind of physical barrier to the anion transport. This fact may be tied to the change in polymer porosity mentioned above. There is no theory available to illustrate the potential and ion concentration changes quantitatively. The above qualitative suggestions can be drawn using the theory for electrode processes of uncharged substrates in the absence of supporting electrolyte.[33] Also, just the formation of the collar may fit well the recent thin layer approach to the electrochemical conversion of insulator to the conductor at the conductor/insulator/electrolyte three-phase interline.[34]

In some cases, the porosity takes the form of very well-defined deep cylinders (see Figure 8A). These cylinders are perpendicular to the electrode surface. Also, under some experimental conditions (in the presence of $KBrO_3$) we found crystalline-like polymer deposits behind the collar. The polymer "crystals" are shown in Figure 8B. They are rather smooth despite the relatively long distance from the phase boundary. An EDX analysis of the polymer crystals (those shown in Figure 8B) indicates that there is an increased level of Br and K in the crystals (5.8 and 9.8 at. %, respectively). At the same time the content of Br (presumably BrO_3^-) was several times lower in the collar and the porous structure compared to the crystals. The elevated contents of ions could be a key factor in the formation of the crystalline-like structure; however, it is not clear how these ions found their way to the crystallization area. This cannot be caused by noticeable solubility of potassium bromate (also as the ion pair) in nitrobenzene; we have made some extraction/conductometric experiments and found the solubility of this salt very limited. Anyway, if the solubility was significant, then the electropolymerization of the monomer could be accomplished along the entire Pt microwire. Therefore, we believe the relatively fast transport of both ions of $KBrO_3$ through the polymer strings, possibly triggered by the electrooxidation of the polymer at the applied potential, is respon-

sible for the elevated concentration of the ions in the crystals. This conclusion is supported by the fact that the crystals sit on the strings.

4. Conclusions

The electrodeposition of a polymer at the three-phase boundary provides two research possibilities. First, it allows the determination of the depth of penetration of anions from the aqueous phase into the organic phase. Second, what is demonstrated for the first time in this paper, such a procedure allows the deposition of polymers in very different forms, such as collars, cylinders, and semicrystals. Behind the variety of polymer forms is the direct contact of the polymer deposit with both: the hydrophobic and the hydrophilic phase. The low anion concentration, the existence of the concentration gradient of the anion, and the potential gradient that develops along the microcylindrical electrode are also responsible for the variations in the polymer structure. Different morphologies of the polymers mean different polymer properties. We believe it might be potentially useful to focus on particular polymer morphology. For example, the polymer deposits with deep cylinders may be useful as membranes protecting the electrode surfaces.

Acknowledgment. Support for this work by the Polish Ministry of Education and Science under Grant Nos. 3T09A 087 27 and 1T09A 118 30 is gratefully acknowledged.

References and Notes

(1) Scholz, F.; Gulaboski, R. *Chem. Phys. Chem*. **2005**, *6*, 16.

(2) Scholz, F.; Schröder, U.; Gulaboski, R. *Electrochemistry of Immobilized Particles and Droplets;* Springer: Berlin, 2004.

(3) Marken, F.; Webster, R. D.; Bull, S. D.; Davies, S. G. *J. Electroanal. Chem.* **1997**, *473*, 209.

(4) Marken, F.; Compton, R. G.; Goeting, Ch. H.; Foord, J. S.; Bull, S. D.; Davies, S. G. *Electroanalysis* **1998**, *10*, 821.

(5) Schröder, U.; Wadhawan, J.; Evans, R. G.; Compton, R. G.; Wood, B.; Walton, D. J.; France, R. R.; Marken, F.; Bulman Page, P. C.; Hayman, C. M. *J. Phys. Chem. B* **2001**, *106*, 8697.

(6) Banks, C. E.; Davies, T. J.; Evans, R. G.; Hignett, G.; Wain, A. J.; Lawrence, N. S.; Wadhawan, J. D.; Marken, F.; Compton, R. G. *Phys. Chem. Chem. Phys.* **2003**, *5*, 4053.

(7) Wadhawan, J. D.; Evans, R. G.; Banks, C. E.; Wilkins, S. J.; France, R. R.; Oldham, N. J.; Fairbanks, A. J.; Wood, B.; Walton, D. J.; Schröder, U.; Compton, R. G. *J. Phys. Chem. B* **2002**, *106*, 9619.

(8) Davies, T. J.; Wilkins, S. J.; Compton, R. G. *J. Electroanal. Chem.* **2006**, *586*, 260.

(9) Ball, J. C.; Marken, F.; Fulian, Q.; Waadhavan, J. D.; Blythe, A. N.; Schroder, U.; Compton, R. G.; Bull, S. D.; Davies, D. G. *Electroanalysis* **2000**, *12*, 1017.

(10) Tasakorn, P.; Chen, J.; Aoki, K. *J. Electroanal. Chem*. **2002**, *533*, 119.

(11) Donten, M.; Stojek, Z.; Scholz, F. *Electrochem. Commun.* **2002**, *4*, 324.

(12) Shul, G.; Opallo, M. *Electrochem. Commun.* **2005**, *7*, 194.

(13) Shul, G.; Opallo, M. *Electrochem. Commun.* **2006**, *7*, 1111.

(14) Rozniecka, E.; Shul, G.; Sirieix-Plenet, J.; Gaillon, L.; Opallo, M. *Electrochem. Commun.* **2005**, *7*, 299.

(15) Shul, G.; Murphy, M. A.; Wilcox, C. D.; Marken, F.; Opallo, M. *J. Solid State Electrochem*. **2005**, *9*, 847.

(16) Li, F.; Chen, Y.; Zhang, M.; Jing, P.; Gao, Z.; Shao, Y. *J. Electroanal. Chem.* **2005**, *579*, 89.

(17) Bak, E.; Donten, M.; Stojek, Z. *Electrochem. Commun.* **2005**, *7*, 483.

(18) Evans-Kennedy, U.; Clohessy, J.; Cunnane, V. J. *Macromolecules* **2004**, *37*, 3660.

(19) Bak, E.; Donten, M. L.; Donten, M.; Stojek, Z. *Electrochem. Commun.* **2005**, *7*, 1098.

(20) Ambrose, J. F.; Nelson, R. F. *J. Electrochem. Soc.* **1968**, *115*, 1159

(21) Dubois, J. E.; Desbene-Monvernay, A.; Lacaze, P. C. *J. Electroanal. Chem.* **1982**, *132*, 177.

(22) Lacaze, P. C.; Dubois, J. E.; Desbene−Monvernay, A.; Desbene, P. L.; Basselier, J. J.; Richard, D. *J. Electroanal. Chem.* **1883**, *147*, 107.

(23) Desbene−Monvernay, A.; Dubois, J. E.; Lacaze, P. C. *J. Electroanal. Chem.* **1989**, *51*, 51.

(24) Skompska, M.; Peter, L. M. *J. Electroanal. Chem.* **1995**, *398*, 57.

(25) Papež, V.; Inganäs, O.; Cimrová, V.; Nešpurek, S. *J. Electroanal. Chem.* **1990**, *282*, 123.

(26) Papež, V.; Novák, P.; Mrha, J. *Z. Phys. Chem. (Muenchen)* **1988**, *160*, 99.

(27) Diaz, A. F.; Bargon, J. In *Handbook of Conducting Polymers*; Skotheim, T., Ed.; Dekker: New York, 1986; p 81.

(28) Skompska, M.; Vorotyntsev, M. A. *J. Solid State Electrochem.* **2004**, *8*, 360−368.

(29) P. Marque, J. Roncali, F. Garnier, J. *Electroanal. Chem.* **1987**, *218*, 107−118.

(30) Weast, R. C., Ed. *Handbook of Chemistry and Physics*, 61st ed.; CRC Press: Boca Raton, FL, 1980; p F-216.

(31) Cong, H. N.; Abbassi, K. E.; Gautier, J. L.; Chartier, P. *Electrochim. Acta* **2005**, *50*, 1369.

(32) Skompska, M.; Kudelski, A. *J. Electroanal. Chem.* **1996**, *403*, 125.

(33) Hyk, W.; Palys, M.; Stojek, Z. *J. Electroanal. Chem*. **1996**, *415*, 13.

(34) Deng, Y.; Wang, D.; Xiao, W.; Jin, X.; Hu, X.; Chen, G. Z. *J. Phys. Chem. B* **2005**, *109*, 14043.